Title

Rectus Extraocular Muscle Paths and Staphylomata in High Myopia.

Authors

Li, Yunping
Wei, Qi
Le, Alan
et al.

Publication Date

2019-05-01

DOI

10.1016/j.ajo.2019.01.029

Peer reviewed

HHS Public Access

Author manuscript

Am J Ophthalmol. Author manuscript; available in PMC 2020 May 01.

Published in final edited form as:

Am J Ophthalmol. 2019 May ; 201: 37–45. doi:10.1016/j.ajo.2019.01.029.

Rectus Extraocular Muscle Paths and Staphylomata in High Myopia

Yunping Li[1,2], **Qi Wei**[3], **Alan Le**[1], **Bola Ayoub Gawargious**[4], and **Joseph L. Demer**[1,4,5,6,7]

[1]Stein Eye Institute and Department of Ophthalmology, University of California, Los Angeles, U.S.A.

[2]Department of Ophthalmology, 2nd Xiangya Hospital, Central South University and Hunan Clinical Research Center of Ophthalmic Disease, Changsha, Hunan, China 410011.

[3]Department of Bioengineering, George Mason University, Fairfax, VA, U.S.A.

[4]Department of Integrative Biology and Physiology, University of California, Los Angeles, U.S.A.

[5]Department of Neurology, University of California, Los Angeles, U.S.A.

[6]Neuroscience Interdepartmental Program, University of California, Los Angeles, U.S.A.

[7]Bioengineering Interdepartmental Program, University of California, Los Angeles, U.S.A.

Abstract

PURPOSE: To investigate the relationship between displacement of extraocular muscles (EOMs) and staphyloma in high myopia using magnetic resonance imaging (MRI).

DESIGN: Retrospective case-control study.

METHODS:

Setting: Institutional Study.

Population: 29 highly myopic patients (46 eyes), 11 age-matched healthy control subjects (21 eyes), and 34 patients (66 eyes) with sagging eye syndrome.

Procedures: MRI was analyzed for aspect ratio (AR) of the ocular cross section, locations of staphylomata and EOMs, and status of superior rectus to lateral rectus (SR-LR) band ligament.

Main Outcome Measures: Association between staphylomata with EOM paths and the LR-SR band.

Corresponding author:Joseph L. Demer, M.D., Ph.D. Stein Eye Institute, 100 Stein Plaza, UCLA, Los Angeles, California, 90095-7002 U.S.A. Phone: 310-825-5931, fax: 310-206-7826, jld@jsei.ucla.edu.

Yunping Li, M.D.,Ph.D., spent one year at Jules Stein Eye Institute, UCLA, as a visiting scholar and now she is working at department of Ophthalmology, 2nd Xiangya Hospital, Central South University and Hunan Clinical Research Center of Ophthalmic Disease, China, 410011

C.*Authorship:* All authors attest that they meet the current ICMJE criteria for authorship.

RESULTS: Several associations of staphylomata were statistically significant (P<0.05). Most staphyloma were superotemporal. Myopic patients with staphyloma had larger ARs in quasi-coronal images than in myopes without staphyloma or normal controls. Compared to high myopes without staphyloma and normal controls, when staphyloma was present, there was more inferior LR displacement, larger LR - globe angle, and larger SR-LR displacement angle than in myopes without staphyloma. Staphyloma in the superotemporal quadrant was associated with greater SR-LR angle than in other quadrants. There were significantly more ruptures of SR-LR band ligament in high myopes with staphyloma than in those without staphyloma.

CONCLUSIONS: Local staphylomata in high myopia reflects ocular asphericity and correlate with EOM paths. Myopic staphylomata are associated with inferior displacement of LR path and defect of the LR-SR band ligament.

High myopia is a leading cause of blindness worldwide, especially in Asia,[1–3] where 2.4 to 4.2% of people over age 30 years have high myopia.[4] Complications of high myopia may be sight-threatening, including the formation of scleral ectasias called staphylomata. While causes of the current myopia epidemic are obscure, high myopia is associated with axial globe elongation and chorioretinal lesions that can represent vision-threatening maculopathies.[5–7]

Staphylomata in high myopia are increasingly common with advancing age.[8–10] Rotation of a staphyloma against an extraocular muscle (EOM) in eccentric gaze can augment mechanical tension in the EOM or displace its path.[10] While there is a paucity of studies investigating the relationship between staphylomata and EOM paths, Demer recently reported that irregular equatorial or posterior staphylomata are common in strabismic axial high myopes, and posited the existence of the “knobby eye syndrome” in which such irregularity in globe contour contributes to strabismus[10]. Yokoyama *et al.* reported that superotemporal displacement of the highly myopic globe in heavy eye syndrome [11], a striking form of acquired pulley heterotopy with limited abduction and supraduction, could disturb EOM paths, yet these authors did not comment on the possible impact of staphylomata.[12] No studies to date have quantitatively explored the relationship between presence of myopic staphyloma and EOM paths.

The present study employed three-dimensional (3D) high-resolution magnetic resonance imaging (MRI)[13] to demonstrate characterize staphylomatous globe deformation in axial high myopia, and to identify the relationship of staphylomata to EOM paths.

METHODS

Subjects

After giving informed consent according to a protocol approved by the Institutional Review Board of the University of California, Los Angeles, and in conformity with the Health Information Portability and Accountability Act and the Declaration of Helsinki, we studied 29 consecutive highly myopic subjects [age 54 ± 17 years (mean ± SD); 10 males and 19 females]. These subjects participated in a prospective MRI study of strabismus at the University of California, Los Angeles, from 1991 to 2016. Eleven age-matched, healthy, orthotropic subjects without myopia (age 61 ± 16 years, 4 males and 7 females, spherical

equivalent is more than −0.50 D) from this study served as normal controls. All subjects underwent visual acuity assessment, motility examination, slit lamp and funduscopic examination, refraction, photography of ocular versions and surface coil MRI of the orbits. High myopia was defined by a spherical equivalent of - 5.00 D or less, or axial length exceeding 26.5 mm measured from MRI if there had been prior cataract or refractive surgery. Axial globe length was determined from high resolution MRI as the distance from the anterior corneal surface to the retinal surface along a line perpendicular to the iris plane, measured in the axial image plane closest to the globe equator. This is as robust approach employed elsewhere[14,15] We also studied another control group consisting of 66 orbits of 34 subjects (age 68 ± 12 years, 15 males and 19 females) clinically diagnosed with sagging eye syndrome (SES) [16] Staphylomata were identified in all groups using MRI.

Magnetic Resonance Imaging

High-resolution T1- or T2-weighted MRI was performed using a 1.5 T scanner (Signa, General Electric, Milwaukee, WI) using published techniques.[10,17] Axial images were obtained in contiguous 2-mm slices over a 10 or 11 cm field of view, yielding 390 pm or 430 mm in-plane resolution. Quasi-coronal images perpendicular to the long axis of each orbit, and quasi-sagittal images parallel to the long axis of each orbit, were obtained at high-resolution (312 μm pixels) in planes of 2 mm thickness in target-controlled central gaze for each eye. The scanned eye was monocularly centered on an afocal, fiberoptic target that does not induce convergence.

Analysis

Images were analyzed using the program *ImageJ64* [18] Ocular shapes were quantitatively described from contiguous axial, quasi-coronal and quasi-sagittal image sets. Left orbits were digitally reflected into the orientation of right orbits, and all orbits corrected for variations in head positioning. Roll rotation was performed first to vertically align the inter-hemispheric fissure of the brain in quasi-coronal images. [19] Axial globe length[6] was measured from axial MRI.[14]

Each eye was first categorized as spherical or nonspherical from MRI in all three planes. Posterior segment curvature was assessed. Staphyloma was defined as an ectasia of the sclera with a local radius of curvature less than that of the surrounding areas in any of the three orthogonal MRI planes.[20] We employed a polar coordinate system in axial and sagittal images to categorize staphyloma location into quadrants: superotemporal, inferotemporal, superonasal, and inferonasal. Counter-clockwise angles were taken as positive.

Classification was made by consensus of two authors (Li and Demer), who were masked to refractive errors and other clinical findings. The traced globe contour was automatically fit to an ellipse in *ImageJ* in the image plane containing the largest globe cross-section including the cornea. As an index of asphericity, aspect ratio was computed as the ratio of the major (long) axis to minor (short) axis length of the ellipse fitted to the globe. Such an approach is independent of ellipse orientation (Fig. 1).[10]

To examine the association between rectus EOM paths and globe shape, we described geometric relationships among orbital structures by several angle measurements. The EOM

displacement angle measures the displacement of horizontal rectus EOMs from the anatomical horizontal line, or of vertical rectus EOMs from the anatomical vertical (midsagittal) line. The angle was calculated between the horizontal or vertical, and a line connecting the respective EOM and globe centroid (Fig. 2). These angles quantify the polar position of each EOM's centroid. The rectus EOM-globe angle measures the EOM's polar angle relative to the elliptical axes of the globe as computed by fitting in *ImageJ.* The angle was then calculated between the major (minor) axis of the globe and the line connecting the horizontal (vertical) rectus EOM and globe centroids (Fig. 3). We found that for the control and the high myopia groups without staphyloma, the globe was close to spherical so that the quasi-coronal aspect ratio was less than 1.05. This caused angular indeterminacy of the fitted ellipses because aspect ratios near 1.0 describe circles, for which major and minor axes cannot be mathematically defined. Therefore, we arbitrarily assigned the major axis to be the cranial horizontal axis for these groups with nearly spherical eyes. Rectus to rectus angles, including the superior rectus (SR) to lateral rectus (LR) angle, the SR to medial rectus (MR) angle, the inferior rectus (IR) to LR angle, and the IR to MR angle, were also measured, analogous to the approach proposed by Yokoyama *et al.* for the SR to LR angle.[12] These angles measure the polar relationships between the respective adjacent rectus EOMs and are obtained from lines connecting the rectus EOM centroid to the globe centroid in quasi-coronal MRI (Fig. 4).

Main outcome measures were quantitative MRI geometry, ocular versions, and binocular alignment. Statistical analyses were performed using GraphPad Prism (GraphPad Software, La Jolla, CA). Significant effects of groups were evaluated using analysis of variance (ANOVA), with subsequent pair-wise contrasts by unpaired t-tests and chi-square tests.

RESULTS

A total of 52 eyes of 32 highly myopic subjects were examined by MRI. Six eyes of three subjects were excluded because of MRI artifacts due to eye movements. Ultimately, 46 eyes of 29 subjects (mean axial length: 29.1± 2.7 mm) were studied. Among these, staphylomata were identified in 17 subjects (29 eyes, mean age 58 ±15 yrs), of whom 8 had strabismus (one with exotropia, four with esotropia, two with HES, one with SES). Among the 12 subjects without staphyloma (17 eyes, mean age 50 ± 20 yrs), of whom 4 had strabismus (two had esotropia, one had SES, and one had HES). There were 21 eyes of 11 age-matched normal controls (mean age 61 ± 16 yrs, axial length 24.1 ± 0.6 mm). There were no significant differences in age and gender distribution among myopic subjects with and without staphyloma, and normal controls. No significant difference in age distribution was found between staphylomatous highly myopic patients with and without SR-LR band rupture (mean age 59 ± 14 vs 53 ± 16 yrs respectively, P = 0.45). Myopic subjects with staphyloma had a longer mean axial length than myopes without staphyloma (mean axial length 29.9 ± 3.0 vs 27.9 ± 1.7 mm respectively, P = 0.02).

Among the 46 highly myopic eyes, 17 (12 patients, 37%), MRI showed no evidence of staphyloma; these eyes were axially elongated, but in spherical or uniformly ellipsoidal shape. There were 35 staphylomata in 29 eyes, including nasally distorted, temporally distorted, cylindrical, or barrel shaped. Diffuse posterior staphylomata were present in 26

eyes, with three exhibiting two distinct staphylomata. Three eyes had both posterior and equatorial staphylomata.

Axial globe aspect ratio was 1.10 ± 0.09 (mean ± SD) in staphylomatous myopes and 1.10 ± 0.05 in non-staphylomatous myopes, both significantly greater than 1.00 ± 0.02 in normal controls (P <0.0001). Aspect ratio in quasi-coronal MRI was 1.10 ± 0.04 in staphylomatous myopes, and 1.00 ± 0.01 in both non-staphylomatous myopes and normal controls. Control subjects had spherical cross sections in quasi-coronal planes as the mean aspect ratio was near unity, as expected. The quasi-coronal aspect ratio of staphylomatous myopes significantly differed from both other groups (P <0.0001).

Displacement angles of the rectus EOMs at the approximate pulley positions are summarized in Fig. 5. The staphylomatous myopes exhibit LR (P = 0.0004) and IR (P = 0.02) displacements significantly different from normal. The inferior displacement of LR in staphylomatous (18 ± 8°) was significantly large r than in non-staphylomatous myopes (12 ± 7° P = 0.03). The IR was also nasally displaced i n non-staphylomatous myopes, indicating association of nasal displacement of IR with high myopia in general. Displacement angles of the SR and MR were similar among groups (P>0.05).

Rectus-globe angles are summarized in Fig. 6. Staphylomatous myopes had significantly larger LR-globe angles (22 ± 9°) than the non-staphylomatous myopes (12 ± 7° P = 0.008) and normal controls (9 ± 5° P<0.0001). The IR-globe angles of the staphylomatous (15 ± 9° P = 0.002) and non-staphylomatous myopes (13 ± 6° P = 0.005) were both significantly higher than the normal controls (8 ± 5°), indicating that nasal displacement of IR is associated with high myopia in general. No other EOM-globe angles differed among groups.

Rectus-rectus displacement angles are presented in Fig. 7. The SR-LR displacement angle in staphylomatous myopes was 109 ± 11° which was significantly greater than in both the normal controls at 97 ± 7° (P < 0.0001) and non- staphylomatous myopes at 101 ± 8°(P = 0.02), with the latter two groups not differing significantly from one another (P = 0.07). The IR-LR displacement angle in staphylomatous myopes was 83 ± 6° which was significantly less than in both normal controls at 89 ± 6°(P = 0.002), and in non-staphyl omatous myopes at 91 ± 9° (P = 0.0009). In general, in staphylomatous myopes there was greater IR and counterclockwise LR displacement, although non-staphylomatous myopes did not differ significantly from normal (P = 0.32). The IR-MR displacement angles in staphylomatous and non-staphylomatous myopes were identical at 74 ± 8°and 74 ± 5° respectively, significantly less than in normal controls at 78 ± 6°(P = 0.04 for both). The SR-MR displacement angles did not differ significantly among groups.

The Table shows that staphylomata were most abundant in the superotemporal quadrant (P=0.002, χ^2 test). The SR-LR displacement angle varied significantly for staphyloma located in different quadrants in high myopes (P = 0.009, one-way ANOVA), being greatest when staphyloma was superotemporal (P = 0.004, t-test).

Status of the SR-LR band is presented in Fig. 8. The SR-LR band was ruptured in 18 of 29 orbits (13 of 17 subjects, 7 of 13 subjects with band ruptured had strabismus including one with SES) in staphylomatous myopes, significantly more than in non-staphylomatous

myopes (P = 0.01), in whom the band was ruptured in only 4 of 17 orbits (3 of 12 subjects, 1 of 3 subjects with band rupture had SES and the other two had no strabismus). This may be compared with SES group, in whom the SR-LR band was defective (ruptured or elongated and attenuated) in all 66 orbits, consistent with prior report.[16] Nine out of 66 orbits with SES exhibited staphylomata, and there was SR-LR band rupture in 7 of these 9. In the 57 orbits with SES but without staphyloma, the SR-LR band was ruptured in 9. Thus, SR-LR band rupture was significantly more likely in the presence of staphyloma (P < 0.0001). Most subjects with SES without staphyloma did not have SR-LR band rupture, but most high myopes with staphylomata did.

DISCUSSION

This study demonstrates that local staphylomata in highly myopic people influence ocular asphericity and are related to EOM positions. The LR is likely to be displaced more inferiorly in staphylomatous than non-staphylomatous high myopes. Staphylomata were particularly common in the superotemporal quadrant, where the SR and LR were more widely separated due to defect of the SR-LR band ligament in this same quadrant. This suggests that the degeneration of orbital connective tissues, especially the LR-SR band, is associated with development of highly myopic staphylomata. Of course, that clear association may or may not be causal, leaving open three possibly interpretations: LR-SR band ligament degeneration might permit staphyloma causation, or staphyloma may cause or accelerate ligament degeneration, or the two phenomena might progress independently under the influence of some common factor. However, additional evidence argues for the possibility that LR-SR band ligament degeneration may promote or accelerate staphyloma formation, as discussed below.

In addition to ordinary forms of strabismus, highly myopic patients can develop three special forms of syndromic strabismus, i.e. “heavy eye syndrome” [11], “sagging eye syndrome” (SES) and “knobby eye syndrome”[10,16,21]. The former is due to inferonasal shift of the LR and nasal shift of the SR paths, both closely opposed to the superotemporally-displaced globe; [22] SES is a less-severe, age-related inferolateral shift of the LR path with generalized elongation of rectus EOM lengths.[21] Previous studies of HES and SES in high myopia did not address the existence of staphyloma. In the present study, there were two subjects with HES and one with SES in who had staphylomatous high myopia; one high myope with SES lacked staphyloma.

Staphylomatous high myopes in the current study exhibited more inferior LR displacement than non-staphylomatous high myopes or normal controls. The mean SR-LR angle in staphylomatous high myopes was larger than in both other groups. The mean SR-LR angle in HES has been reported to be 121± 7° and in SES 104 ± 11° [21] The mean SR-LR angle (109 ± 11°) in staphylomatous high myopes here is intermediate between HES and SES. While most staphylomata were located in the superotemporal and inferotemporal quadrants, the SR-LR angle was significantly larger with supratemporal than inferotemporal staphylomata (P = 0.04).

Aging is associated with degeneration of the orbital connective tissue bands that couple the pulleys to one another.[23,24] The SR-LR band originates from the lateral border of the SR pulley and terminates in the superior border of the LR pulley.[24] The SR-LR band typically degenerates in elderly people, allowing inferior displacement of the LR pulley and eOm.[6,25–27] Subject groups in the current study were all similarly elderly. There was significantly more frequent LR-SR rupture in staphylomatous than non-staphylomatous high myopes. Although attenuation and elongation of the LR-SR band were common in subjects with SES, the more extreme form of SR-LR band rupture was significantly more likely when staphyloma was also present. This indicates LR-SR degeneration is more likely to be severe when associated with staphylomata.

We suppose three main possibilities for the association of LR-SR band degeneration with staphyloma in high myopia. One possibility is that LR-SR band degeneration may allow superotemporal staphylomata to form and progress due to absence of inward mechanical pressure of the band against the sclera. In the absence of such ligamentous pressure against the superotemporal sclera, it might bulge under the unopposed influence of intraocular pressure. Thus, pulley ligament disease might be a permissive cause of staphyloma formation. Alternatively, the superotemporal staphyloma may bulge against the LR-SR band and mechanically accelerate its degeneration. A third possibility is that development of staphyloma in high myopia is related generalized connective tissue weakness, that may accelerate both scleral and LR-SR band stretching and attenuation. The third possibility of general tendency for connective tissue weakness would, however, not explain why the superotemporal quadrant is especially susceptible, arguing instead for a role of local anatomical and mechanical factors related to the extraocular muscles. If the first possibility that the LR-SR ligament restrains staphyloma formation proves correct, then surgical or photochemical cross-linking repair of the LR-SR ligament might represent options for treatment or prophylaxis of staphylomata. Regardless of the foregoing etiological considerations, ophthalmic surgeons who treat high myopes with HES or SES should be aware that superotemporal staphylomata are likely to be present, and plan accordingly.

There are limitations to this study. First, it included highly myopic patients who attended a tertiary referral center, so results may not represent the general population. Second, there were small numbers of axial high myopes and subjects with staphyloma. We employed strict inclusion criteria to assess the exclusive influence of axial high myopia, constituting a study strength but decreasing the sample size. There currently exists no adequate biomechanical model to generally compute the effects of irregular staphylomata generally; all existing models of binocular alignment, the most complete being *Orbit 1.8,* assume a spherical globe.[28] Consequently, we cannot provide a quantitative analysis of the potential mechanical interactions among the EOMs, orbital connective tissues, and the globe.

In conclusion, the present results clearly demonstrate a novel relationship between staphylomata, EOM displacement, and LR-SR band ligament degeneration in axial high myopes. The association between SR-LR band degeneration and equatorial or posterior staphyloma in high myopia may suggest future strategies for prevention and management of staphylomata, which are major contributors to sight-threatening complications of myopia.

ACKNOWLEDGEMENTS/DISCLOSURES

A. *Funding/Support:* Grants EY008313 and EY000331 from the US Public Health Service, National Eye Institute and an unrestricted grant from Research to Prevent Blindness. The sponsors or funding organizations had no role in the design or conduct of this research.

B. *Financial Disclosures:* Joseph L. Demer: National Eye Institute Grant EY008313 and an Unrestricted Grant to the UCLA Department of Ophthalmology from Research to Prevent Blindness. The following authors have no financial disclosures: Yunping Li, Qi Wei, Alan Le, and Bola Ayoub Gawargious.

REFERENCES

1. Lin LL, Shih YF, Hsiao CK, Chen CJ. Prevalence of myopia in Taiwanese schoolchildren: 1983 to 2000. Ann Acad Med Singapore. 2004;33(1):27–33.
2. Kim EC, Morgan IG, Kakizaki H, Kang S, Jee D. Prevalence and risk factors for refractive errors: Korean National Health and Nutrition Examination Survey 2008–2011. PLoS One. 2013;8(11):e80361. [PubMed: 24224049]
3. Holden BA, Fricke TR, Wilson DA, et al. Global Prevalence of Myopia and High Myopia and Temporal Trends from 2000 through 2050. Ophthalmology. 2016;123(5): 1036–1042. [PubMed: 26875007]
4. Verkicharla PK, Ohno-Matsui K, Saw SM. Current and predicted demographics of high myopia and an update of its associated pathological changes. Ophthalmic Physiol Opt. 2015;35(5):465–475. [PubMed: 26303444]
5. Hayashi K, Ohno-Matsui K, Shimada N, et al. Long-term pattern of progression of myopic maculopathy: a natural history study. Ophthalmology. 2010;117(8):1595–1611, 1611 e1591–1594. [PubMed: 20207005]
6. Ohno-Matsui K, Kawasaki R, Jonas JB, et al. International photographic classification and grading system for myopic maculopathy. Am J Ophthalmol. 2015; 159(5):877–883 e877. [PubMed: 25634530]
7. Ohno-Matsui K, Lai TY, Lai CC, Cheung CM. Updates of pathologic myopia. Prog Retin Eye Res. 2016;52:156–187. [PubMed: 26769165]
8. Hsiang HW, Ohno-Matsui K, Shimada N, et al. Clinical characteristics of posterior staphyloma in eyes with pathologic myopia. Am J Ophthalmol. 2008;146(1):102–110. [PubMed: 18455142]
9. Gupta P, Cheung CY, Saw SM, et al. Peripapillary choroidal thickness in young Asians with high myopia. Invest Ophthalmol Vis Sci. 2015;56(3):1475–1481. [PubMed: 25655797]
10. Demer JL. Knobby Eye Syndrome. Strabismus. 2018;26(1):33–41. [PubMed: 29279023]
11. Wong TY, Ferreira A, Hughes R, Carter G, Mitchell P. Epidemiology and disease burden of pathologic myopia and myopic choroidal neovascularization: an evidence-based systematic review. Am J Ophthalmol. 2014;157(1):9–25 e12. [PubMed: 24099276]
12. Yokoyama T, Tabuchi H, Ataka S, Shiraki K, Miki T, Mochizuki K. The mechanism of development in progressive esotropia with high myopia In: de Faber JT, ed. Transactions of the 26th meeting of European Strabismological Association. Barcelona, Spain, 9 2000 Lisse (Netherland): Swets & Zeitlinger Publishers; 2000:218 −221.
13. Singh KD, Logan NS, Gilmartin B. Three-dimensional modeling of the human eye based on magnetic resonance imaging. Invest Ophthalmol Vis Sci. 2006;47(6):2272–2279. [PubMed: 16723434]
14. Demer JL. Optic Nerve Sheath as a Novel Mechanical Load on the Globe in Ocular Duction. Invest Ophthalmol Vis Sci. 2016;57(4):1826–1838. [PubMed: 27082297]
15. Bencic G, Vatavuk Z, Marotti M, et al. Comparison of A-scan and MRI for the measurement of axial length in silicone oil-filled eyes. The British journal of ophthalmology. 2009;93(4):502–505. [PubMed: 19074920]
16. Chaudhuri Z, Demer JL. Sagging eye syndrome: connective tissue involution as a cause of horizontal and vertical strabismus in older patients. JAMA Ophthalmol. 2013; 131 (5):619–625. [PubMed: 23471194]

17. Demer JL, Dushyanth A. T2-weighted fast spin-echo magnetic resonance imaging of extraocular muscles. J AAPOS. 2011;15(1):17–23. [PubMed: 21397801]
18. Rasband W ImageJ. US National Institutes of Health1997–2014.
19. Clark RA, Miller JM, Demer JL. Three-dimensional location of human rectus pulleys by path inflections in secondary gaze positions. Invest Ophthalmol Vis Sci. 2000;41(12):3787–3797. [PubMed: 11053278]
20. RF S Staphyloma: Part 1 In: Pathologic myopia. New York, NY: Springer; 2013.
21. Tan RJ, Demer JL. Heavy eye syndrome versus sagging eye syndrome in high myopia. J AAPOS. 2015;19(6):500–506. [PubMed: 26691027]
22. Yamaguchi M, Yokoyama T, Shiraki K. Surgical procedure for correcting globe dislocation in highly myopic strabismus. Am J Ophthalmol. 2010;149(2):341–346.e342. [PubMed: 19939345]
23. Demer JL. More respect for connective tissues. J AAPOS. 2008;12(1):5–6. [PubMed: 18314070]
24. Kono R, Poukens V, Demer JL. Quantitative analysis of the structure of the human extraocular muscle pulley system. Invest Ophthalmol Vis Sci. 2002;43(9):2923–2932. [PubMed: 12202511]
25. Rutar T, Demer JL. “Heavy Eye” syndrome in the absence of high myopia: A connective tissue degeneration in elderly strabismic patients. J AApOs. 2009;13(1):36–44. [PubMed: 18930668]
26. Clark RA, Isenberg SJ. The range of ocular movements decreases with aging. J AAPOS. 2001;5(1):26–30. [PubMed: 11182669]
27. Clark RA, Demer JL. Effect of aging on human rectus extraocular muscle paths demonstrated by magnetic resonance imaging. Am J Ophthalmol. 2002; 134(6):872–878. [PubMed: 12470756]
28. Miller JM PD, Shaemeva I. Orbit 1.8 Gaze Mechanics Simulation. San Francisco: Eidactics; 1999.

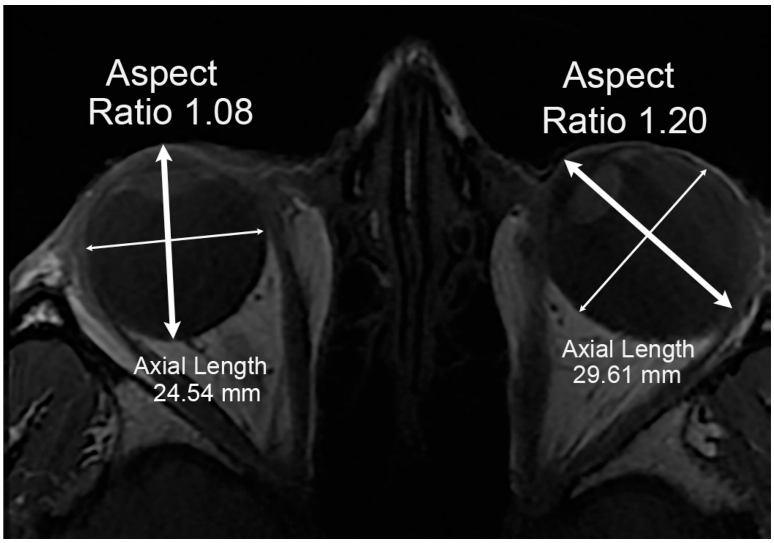

Fig. 1.

Axial MRI of esotropic subject with left unilateral axial myopia. Major axes of ellipses fitting each globe cross section are indicated by bold bidirectional arrows and minor axes by thin arrows. Emmetropic right eye cross section is nearly circular even including the cornea for aspect ratio 1.08, while cross section of diffusely staphylomatous, myopic left eye is oval with aspect ratio 1.20. Axial length of the myopic left eye is about 5 mm greater than emmetropic right eye.

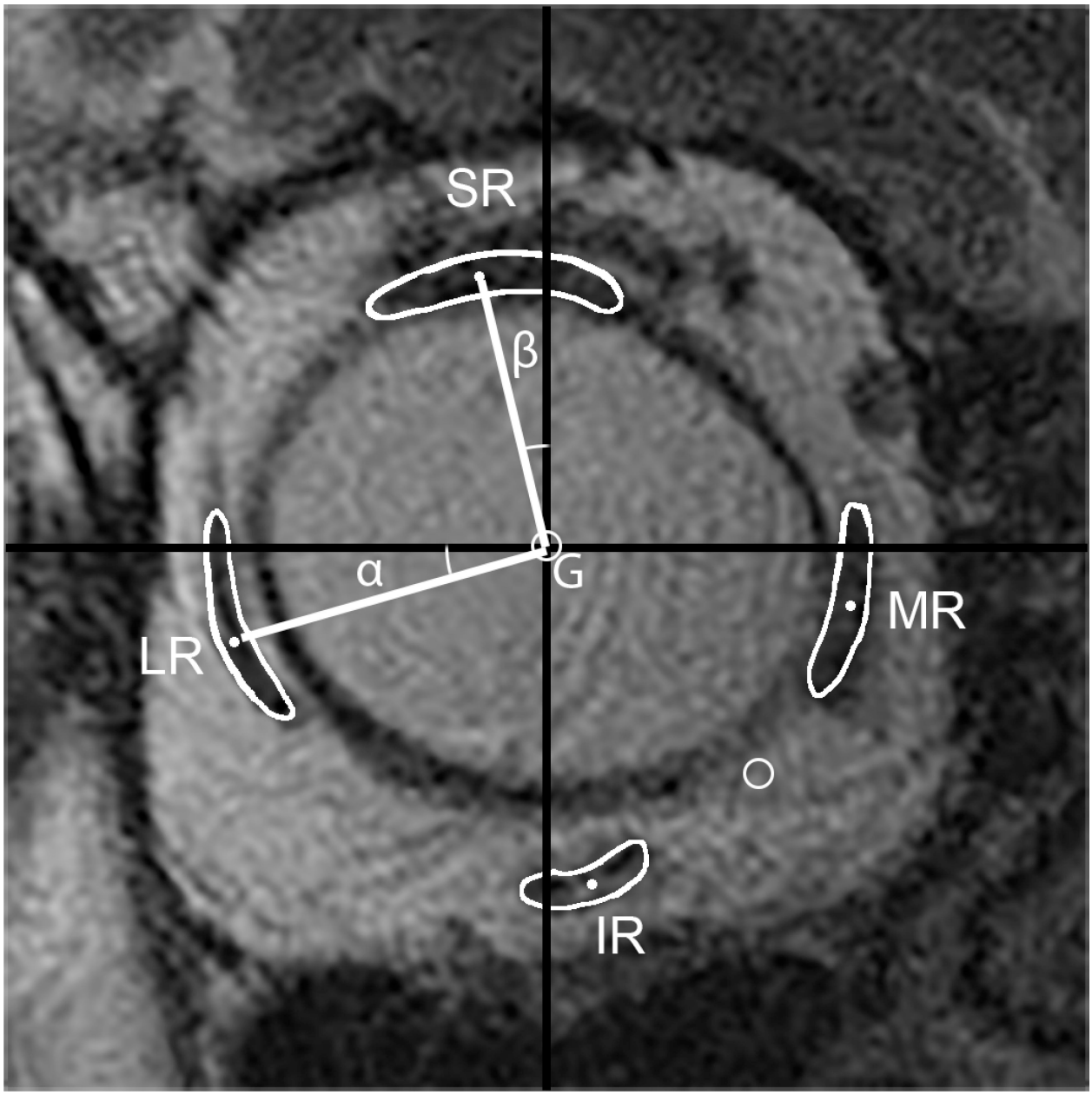

Fig. 2.

Quasi-coronal MRI of right orbit of highly myopic subject, 4 mm posterior to the largest globe cross section, illustrating the lateral rectus (LR) angle (α) to the horizontal, and the superior rectus (SR) angle to the vertical (β), formed with white lines connecting the centroids (white dots) of the respective muscles. Globe centroid is designated G. MR, medial rectus muscle; IR, inferior rectus muscle.

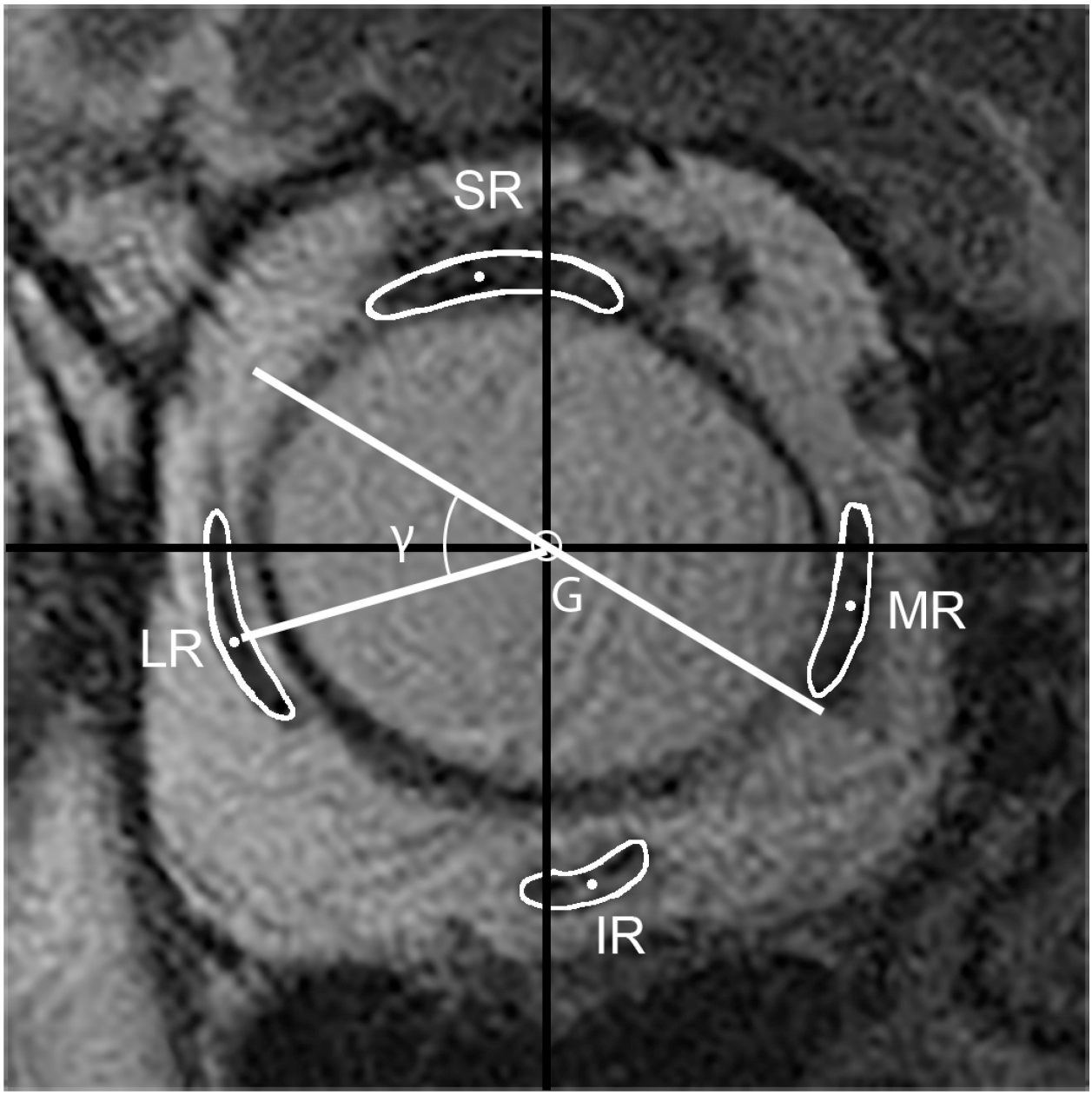

Fig. 3.

Quasi-coronal MRI of right orbit of the highly myopic subject illustrated in Fig. 2, but marked to illustrate lateral rectus (LR) - globe angle (γ), formed by white line between the centroids (white dots) of muscle and globe (G), and the major axis of the ellipse best fitting the globe. SR, superior rectus muscle; MR, medial rectus muscle; IR, inferior rectus muscle.

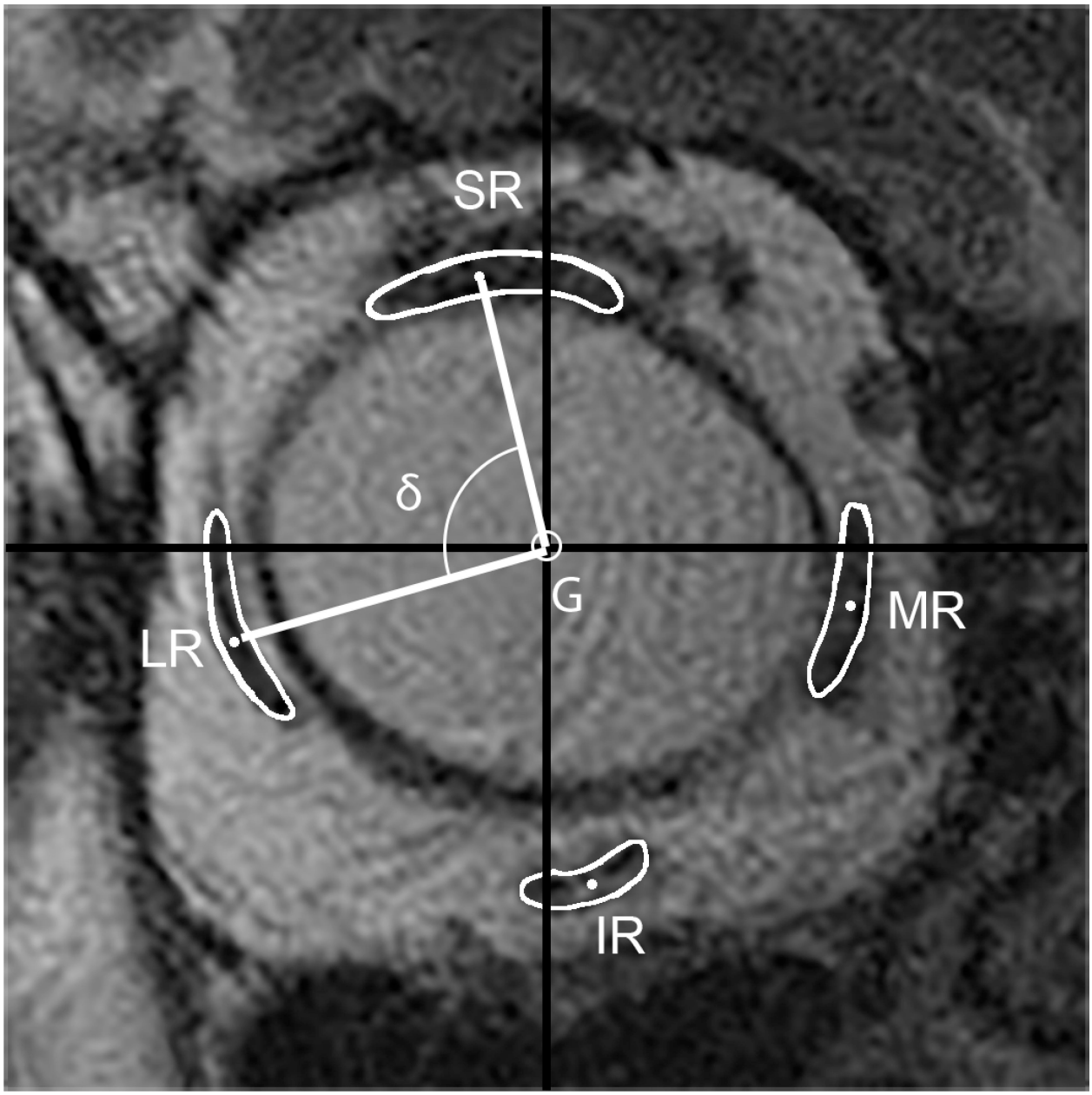

Fig. 4.

Quasi-coronal MRI of the right orbit of the highly myopic subject illustrated in Fig. 2, but marked to illustrate the superior rectus (SR) - lateral rectus (LR) angle (δ), formed by lines connecting the centroids (white dots) of the SR and globe (G), with the line connecting the centroids of the globe and the LR. MR, medial rectus muscle; IR, inferior rectus muscle.

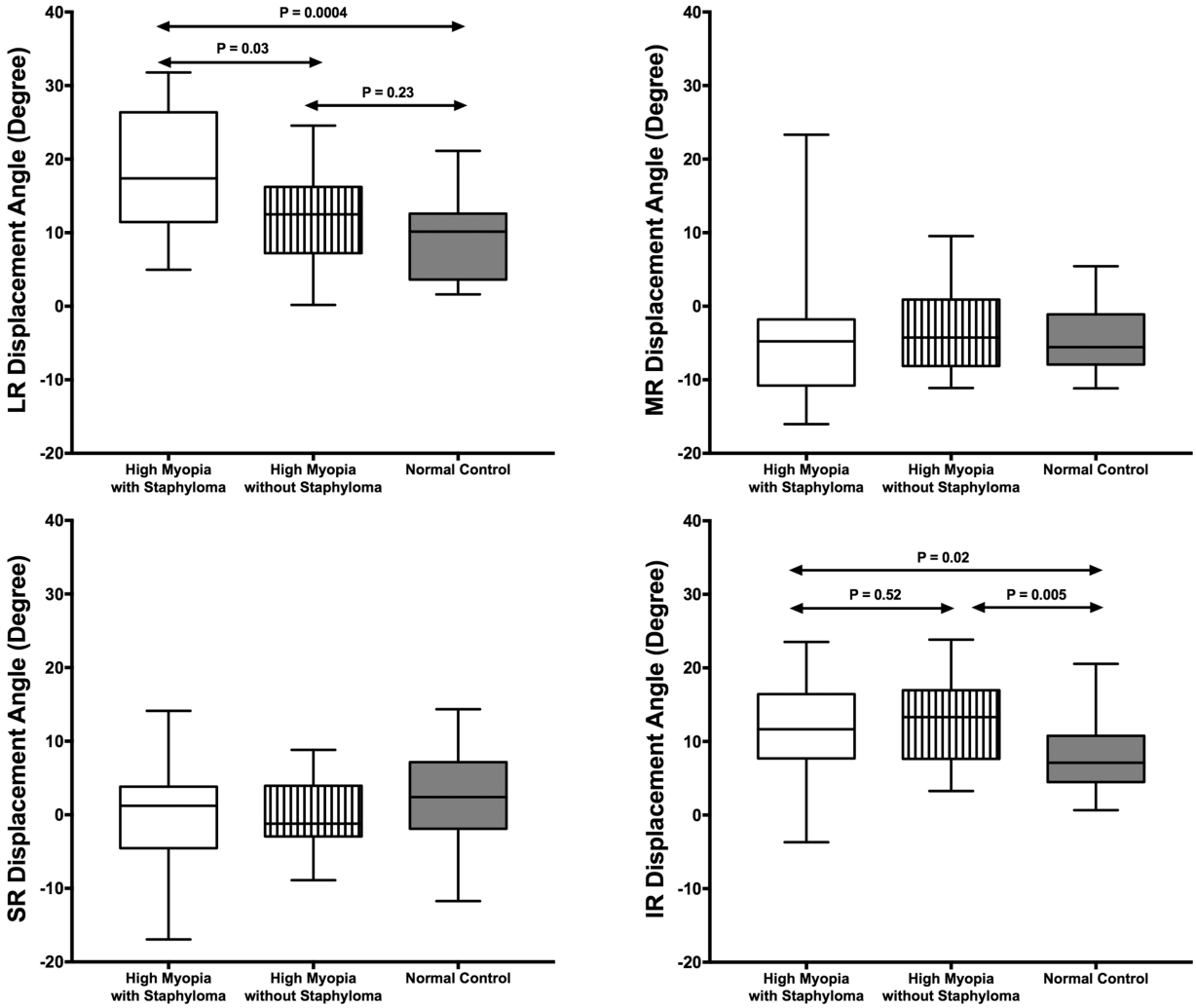

Fig. 5.

Displacement of horizontal rectus EOMs from the anatomical horizontal line, or of vertical rectus EOMs from the anatomical vertical (midsagittal) line, counter-clockwise positive. Horizontal bars indicate the median, rectangles the interquartile range, and error bars the minimum and maximum values. LR = lateral rectus; MR = medial rectus; SR = superior rectus; IR = inferior rectus.

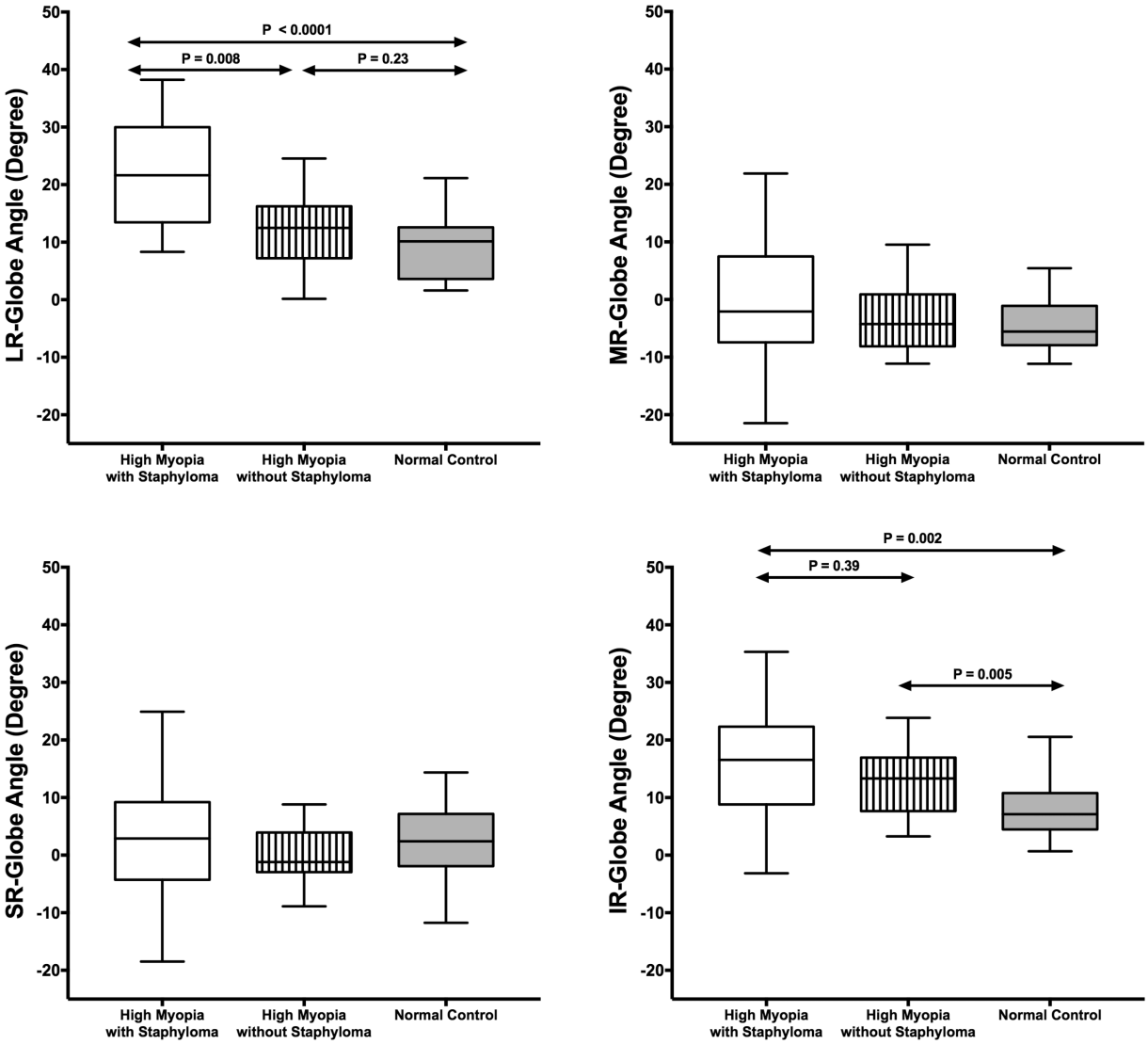

Fig. 6.

Angle between the major (minor) axis of the globe and the polar angle to from the horizontal (vertical) rectus EOM centroid to the globe centroid. Conventions and abbreviations as in Fig. 5.

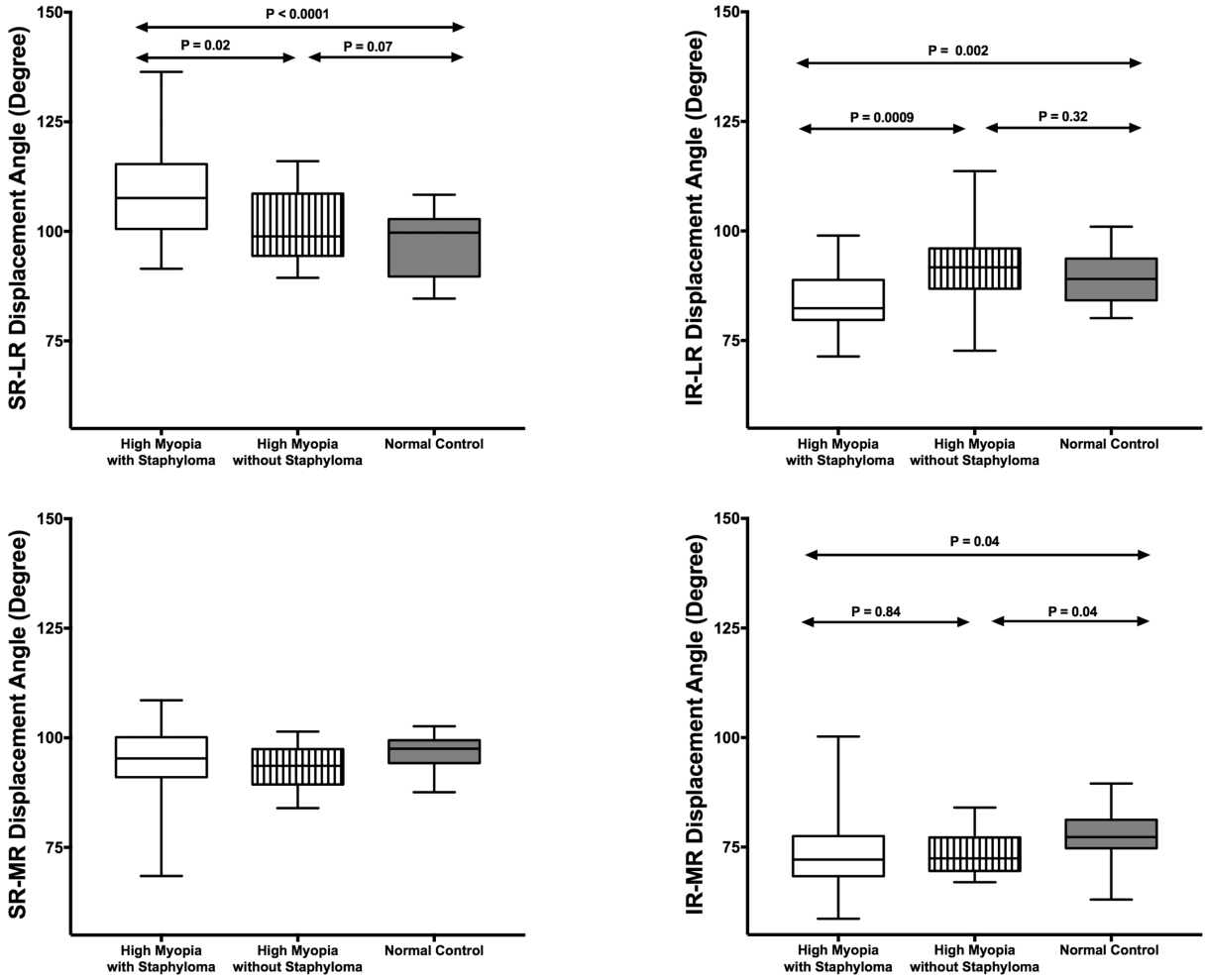

Fig. 7.

Polar relationships between the respective adjacent rectus muscles, from lines connecting muscle centroids to globe centroid in quasi-coronal MRI. Conventions and abbreviations as in Fig. 5.

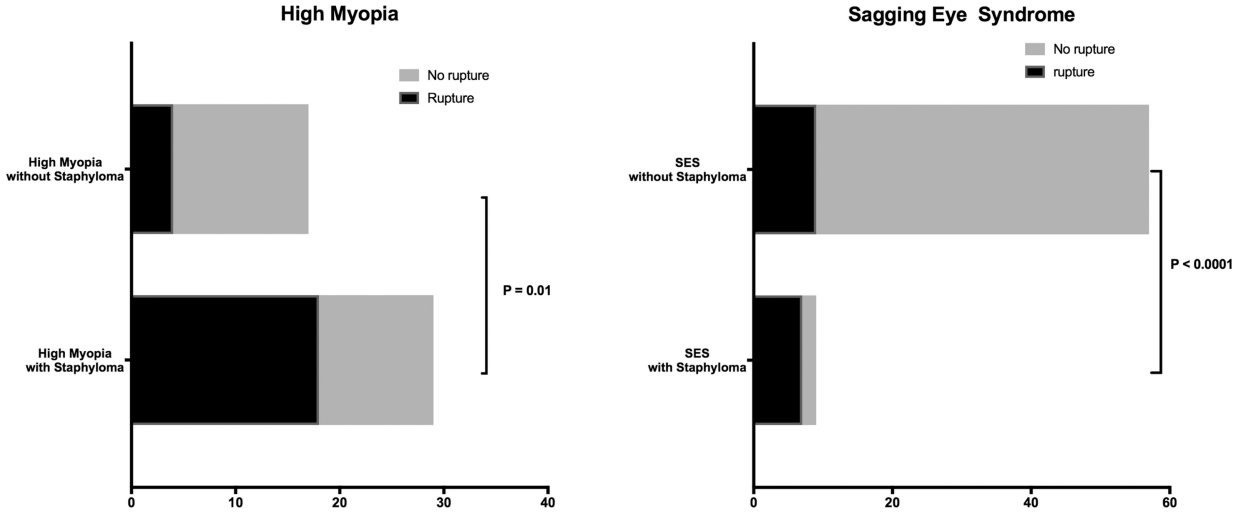

Fig. 8.

Distribution of SR-LR band rupture in high myopia and sagging eye syndrome (SES) with and without staphyloma, with axis indicating number of cases. LR = lateral rectus; SR = superior rectus.

Table.

Quadrant Comparison of Staphylomata and SR-LR Angle

Quadrant	Supero-temporal	Infero-temporal	Supero-nasal	Infero-nasal	P-Value
Number of staphyloma	16	10	6	3	0.002 [a]
SR-LR angle	114 ± 11°	105 ± 8°	100 ± 12°	105 ± 8°	0.009 [b]

[a] Chi-square test

[b] One-way analysis of variance

SR = superior rectus muscle; LR = lateral rectus muscle